Journal of Applied Polymer Science

Effect of 1-butyl-3-methylimidazolium iodide containing electrospun poly(vinylidene fluoride-*co*-hexafluoropropylene) membrane electrolyte on the photovoltaic performance of dye-sensitized solar cells

E. Vijayakumar,[1] A. Subramania,[1] Zhaofu Fei,[2] Paul J. Dyson[2]

[1]Electrochemical Energy Research Lab, Centre for Nanoscience and Technology, Pondicherry University, Puducherry 605 014, India

[2]Institut des Sciences et Ingénierie Chimiques, Ecole Polytechnique Fédérale de Lausanne (EPFL), CH-1015, Lausanne, Switzerland

Correspondence to: A. Subramania (E-mail: a.subramania@gmail.com)

ABSTRACT: Electrospun poly(vinylidene fluoride-*co*-hexafluoropropylene) (PVdF-HFP) membrane was prepared from a solution of 16 wt % of PVdF-HFP containing acetone/*N*,*N*-dimethyl acetamide (7 : 3 wt %). The prepared electrospun PVdF-HFP membrane (esPM) was then soaked in ionic liquid electrolyte containing 0.5*M* LiI, 0.05*M* I_2, and 0.5*M* 4-tert butylpyridine, 0.5*M* 1-butyl-3-methylimidazolium iodide (BMImI) in acetonitrile to get electrospun PVdF-HFP membrane electrolyte (esPME). The effect of various concentrations of BMImI containing esPME on ionic conductivity was studied by AC-impedance measurements and the I^-/I_3^- diffusion co-efficients was determined by linear sweep voltammetry. The photovoltaic performance of a DSSC fabricated using 0.5*M* BMImI containing electrospun PVdF-HFP membrane electrolyte (0.5*M* BMImI-esPME) has power conversion efficiency (PCE) of 6.42%. But the stability of the DSSC fabricated using 0.5*M* BMImI-esPME was considerably superior to that fabricated using 0.5*M* BMImI containing liquid electrolyte (0.5*M* BMImI-LE). © 2015 Wiley Periodicals, Inc. J. Appl. Polym. Sci. **2015**, *132*, 42032.

KEYWORDS: electrospinning; fibers; ionic liquids; membranes; photochemistry

Received 14 October 2014; accepted 26 January 2015
DOI: 10.1002/app.42032

INTRODUCTION

Ionic liquid (IL) electrolytes are widely used in dye-sensitized solar cells (DSSCs) in place of organic electrolytes as they are nonvolatile and thermally stable.[1–3] Nonetheless, DSSCs based on ILs are prone to leakage, and in order to overcome this problem, polymer gel electrolytes have been developed for DSSCs.[4–6] Although polymer gel electrolyte-based DSSCs do not suffer from electrolyte loss, they tend to have low power conversion efficiencies attributed to the lower ionic mobility of I^-/I_3^- ions. To improve the photovoltaic efficiency of DSSCs, 1-butyl-3-methylimidazolium iodide (BMImI) has been evaluated as polymer electrolyte additive to enhance the physical diffusion of I^- and I_3^- ions.[7,8] Polymer electrolytes can be prepared by a number of processing techniques including drawing, template synthesis, casting, phase separation, and electrospinning.[9–14] Among these, electrospinning is a simple and cost-effective technique for producing electrospun polymer membranes that affords an average fiber diameter in the submicron range with high porosity, large surface area, and a fully interconnected pore structure with good mechanical strength. In recent years, many efforts have been made to improve the photovoltaic performance of DSSCs by improving the ionic conductivity of polymer membrane electrolytes. The effect of 1,2-dimethyl-3-propyl imidazolium iodide (DMPImI) and 1-propyl-3-methyl imidazolium iodide (PMImI) on electrospun poly(vinylidene fluoride-*co*-hexafluoropropylene) (PVdF-HFP) membrane electrolytes have been studied in dye-sensitized solar cells (DSSCs).[15–17] Recently, BMImI-based ionic liquid electrolytes have been used to evaluate the performance of newer counter electrode materials for DSSCs.[18–22] The effect of 1,2-dimethyl-3-propyl imidazolium iodide (DMPImI) and 1-propyl-3-methyl imidazolium iodide (PMImI) containing electrospun poly(vinylidene fluoride-*co*-hexafluoropropylene) (PVdF-HFP) membrane electrolytes on photovoltaic performance of DSSCs have been reported so far. But there is no report on the effect of 1-butyl-3-methylimidazolium iodide (BMImI) containing electrospun PVDF-HFP membrane electrolyte on the photovoltaic performance of DSSCs. Hence, in the present investigation, the effect of various concentrations of BMImI containing electrospun PVDF-HFP membrane electrolytes on the photovoltaic performance of DSSC is studied in detail.

EXPERIMENTAL

Materials

1-Butyl-3-methyl imidazolium iodide was prepared as per the literature protocol.[23] Acetone, *N*,*N*′-dimethylacetamide were procured from Merck India Ltd. Lithium iodide, iodide, 4-*tert*-butylpyridine, acetonitrile were procured from Sigma Aldrich and PVdF-HFP from Arkema (Kynar flex 2801). All these chemicals are analytical grade and used as received without any further purification.

Preparation of Electrospun PVDF-HFP Membrane (esPM)

The esPM was prepared from a solution of 16 wt % of PVdF-HFP in a mixture of acetone/*N*,*N*′-dimethyl acetamide (7 : 3 wt %) as described previously. The resultant nanofibrous mat was vacuum-dried at 80°C for 12 h to remove residual solvent. The thickness of esPM was reduced from about 30 to 20 μm by hot pressing.[13]

Characterization of Electrospun PVdF-HFP Membrane

The surface morphology of esPM was examined using scanning electron microscopy (Hitachi, Model S-4200) under vacuum. The porosity (P) of esPM was determined by weighing the membrane with and without 1-butanol and applying the following equation:[24]

$$P=\frac{m_a/\rho_a}{m_a/\rho_a+m_p/\rho_p} \quad (1)$$

where m_a is the weight of esPM after impregnation with 1-butanol, m_p is the weight of esPM before impregnation with 1-butanol, and ρ_a and ρ_p are density of 1-butanol and the dried esPM, respectively. The density of pure PVdF-HFP is 1.77 g cm^{-3}.

To measure the electrolyte uptake of the esPM, the esPM was soaked in the ionic liquid electrolyte containing 0.5*M* BMImI, 0.5*M* LiI, 0.05*M* I_2, and 0.5*M* 4-*tert*-butylpyribine in acetonitrile for 24 h. The resulting esPME was removed and excess electrolyte solution on the membrane was removed by wiping. Electrolyte uptake (U) was estimated using the formula:

$$U\ (\%)=[(m-m_\circ)/m_\circ]\times 100 \quad (2)$$

where m and m_o are the mass of wet and dry esPM, respectively.

The leakage of the electrolyte was calculated using the equation:[25,26]

$$R=\frac{M_{PE}}{M_{PE,saturated}} \quad (3)$$

where R is the relative absorption of the liquid electrolyte, $M_{PE,saturated}$ is the mass of the polymer electrolyte when the membrane is fully saturated with the liquid electrolyte, and M_{PE} is the mass of the polymer electrolyte after a time interval, when the saturated polymer membrane electrolyte is squeezed by pressing it between two pieces of filter paper.

The effect of various concentrations of BMImI (0.1–0.7*M*) in the liquid electrolyte on the diffusion coefficient of I^-/I_3^- was determined by linear sweep voltammetry in the potential range −0.8 to 0.8 V (vs. SCE) using a conventional three electrode system, consisting of a standard calomel electrode as the reference electrode, Pt foil as the counter electrode, and a Pt microelectrode as the working electrode at 5 mV s^{-1}. The diffusion coefficient (D) of I^-/I_3^- was calculated from the cathodic and anodic steady state current (I_{ss}) using the following equation:[27,28]

$$I_{ss}=4nCrFD \quad (4)$$

where n is the electron number per molecule, F is the Faraday constant, C is the bulk concentration of electroactive species and r is the radius of gold microelectrode, and D is the diffusion coefficient.

The esPMs were soaked in the liquid electrolyte containing various concentrations of BMImI to afford the corresponding esPMEs.[13] The ionic conductivities (σ) of the resultant esPMEs were measured by sandwiching each esPME between two stainless steel blocking electrodes and applying the AC-impedance technique (Biologic Model: VSP) at 25°C. Analysis of these spectra yields information about the properties of esPMEs such as the membrane resistance (R). The membrane resistance associated with the impedance plot with real axis was determined. The ionic conductivity (σ) of the esPMEs was calculated using the equation:

$$\sigma=\ell/RA \quad (5)$$

where ℓ is the polymer membrane thickness, A is the area of the esPME, and R is the resistance of the esPME. The frequency limit was set between 1 mHz and 100 KHz with an AC amplitude of 10 mV. The thickness (ℓ) of the esPME was determined using a digital micrometer and was found to be 20 μm. The area (A) of the esPME was 1 cm^2. The Tafel polarization curves of the fabricated symmetrical cells, i.e. ITO/Pt/BMImI-esPME/Pt/ITO were measured using electrochemical work station (Biologic, Model: VSP) to study the electrocatalytic activity of esPMEs.

Fabrication of DSSCs

The DSSCs were fabricated following a literature procedure;[13] FTO glass plates were cleaned with acetone, ethanol, and then deionized water in an ultrasonic water bath and dried in air. Scotch tape was employed as a spacer to control the film thickness and to provide uncoated areas for electrical contact. Titania paste (Dyesol Ltd.) was spread over the spacer between the scotch tape on the conducting glass substrate using the doctor blade technique. The TiO_2 coating was then dried in air at 30°C for 10 min and sintered at 450°C in air at the rate of 5°C min^{-1} for 30 min to remove any organic matter. The thickness of the photoanode film was about 10 to 12 μm and its area was 0.20 cm^2. After cooling to 80°C the TiO_2 electrodes were immersed into purified 0.3 m*M* ditetrabutylammonium*cis-bis* (isothiocyanato) *bis* (2,2′-bipyridyl-4,4′-bicarboxylato)ruthenium(II) (N719 dye, Sigma Aldrich) solution for 12 h at 30°C.[29] After the dye adsorption the films were cleaned with pure ethanol to remove the excess dye and dried with hot air. For the counter electrode, small holes were drilled on the FTO plates using a micro driller and washed with 0.1*M* HCl solution in ethanol and then cleaned in an ultrasonic bath with detergent solution, ethanol and acetone for 20 min. A Pt counter electrode was prepared by spreading platinum paste (Dyesol Ltd.) in the space between the scotch tape on the conducting glass substrate using the doctor blade technique, followed by drying

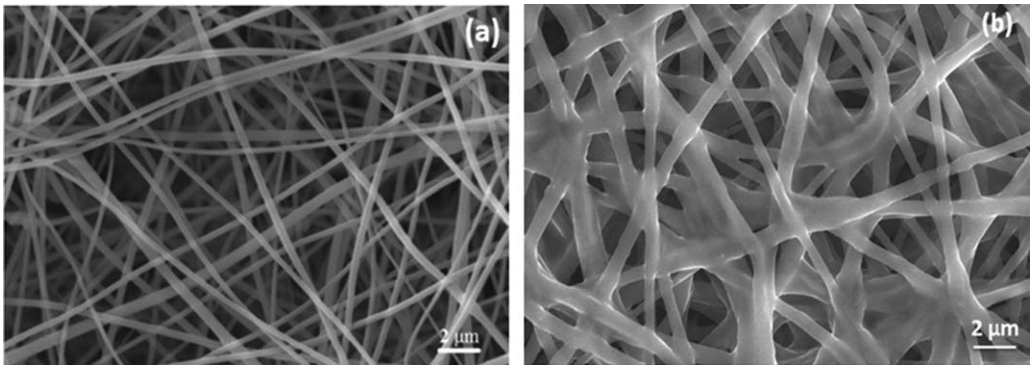

Figure 1. SEM image of the a) esPM and b) esPME.

and then sintered at 450°C for 30 min at the heating rate of 5°C min^{-1}. The thickness of the counter electrode was about 8 to 10 μm. The DSSC was fabricated using 0.5*M* BMImI-esPME by sandwiching a slice of it in between a dye-sensitized TiO_2 photoanode and Pt counter electrode. The dye adsorbed titania photoanode and Pt counter electrode were assembled using 60 μm hot melt thermoplastic sealer (Surlyn). Similarly, a DSSC based on 0.5*M* BMImI-LE was also fabricated for comparison.

Photovoltaic Performance of the DSSCs

The performance of the DSSCs was determined using a calibrated AM 1.5 solar simulator (Newport, Oriel instruments, Model: 67005) with a light intensity of 100 mW cm^{-2} and a computer controlled digital source meter (Keithley, Model: 2420). The *I–V* measurements were carried out on the DSSCs after an aging period of 24 h. Thermally sealed cells were stored in a desiccator and applied to electrochemical measurements every 48 h in order to study their long term stability. The photoelectrochemical parameters, i.e., the fill factor (FF) and light-to-electricity conversion efficiency (η), were calculated with the following equations:[30]

$$\eta\ (\%) = \frac{V_{max} J_{max}}{P_{in}} \times 100 \quad = \frac{V_{oc} J_{sc} FF}{P_{in}} \times 100 \qquad (6)$$

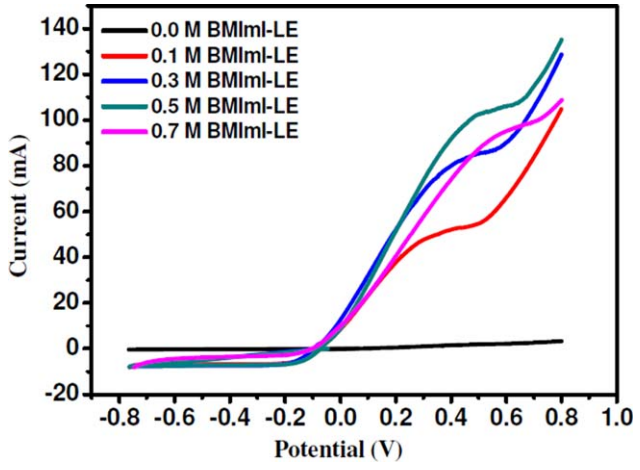

Figure 2. Linear sweep voltammograms for various concentrations of BMImI containing LEs. [Color figure can be viewed in the online issue, which is available at wileyonlinelibrary.com.]

$$FF = \frac{V_{max} J_{max}}{V_{oc} J_{sc}} \qquad (7)$$

where J_{sc} is the short-circuit current density (mA cm^{-2}), V_{oc} is the open-circuit voltage (V), P_{in} is the incident light power (mW cm^{-2}), and J_{max} and V_{max} are the current density (mA cm^{-2}) and voltage (V) in the *J–V* curves, respectively, at the point of maximum power output. All the fabrication steps and characterization measurements were carried out in an ambient environment without a protective atmosphere. The photovoltaic parameter values were made by taking average values of three DSSCs for each system.

RESULTS AND DISCUSSION

Morphology, Porosity, and Electrolyte Uptake

The morphology of the prepared esPM and esPME was characterized by SEM (Figure 1). The esPM has a three-dimensional network structure with a high porosity and fully interconnected pores capable of incorporating large amounts of ionic liquid electrolyte that should improve the electrocatalytic activity of iodide and triodide redox reaction. The membrane presumably has good mechanical strength due to the three dimensional network structure and cross linking points. The esPM (average diameter of the fibers is 350–400 nm) has maximum porosity of 89% with an electrolyte uptake of 340% and a very low solution leakage of 0.3%.

Diffusion Coefficient Studies

The cathodic and anodic steady state currents (I_{ss}) for triiodide and iodide were determined for liquid electrolytes containing

Table I. Diffusion Coefficient of Triiodide and Iodide as a Function of Various Concentrations of BMImI in the Liquid Electrolyte

Electrolyte	Diffusion coefficient of triiodide ($\times 10^{-4}$ cm^2 S^{-1})	Diffusion coefficient of iodide ($\times 10^{-5}$ cm^2 S^{-1})
0.0*M* BMIml-LE	0.13	0.25
0.1*M* BMIml-LE	4.78	5.95
0.3*M* BMIml-LE	7.50	6.26
0.5*M* BMIml-LE	9.05	6.53
0.7*M* BMIml-LE	8.55	3.10

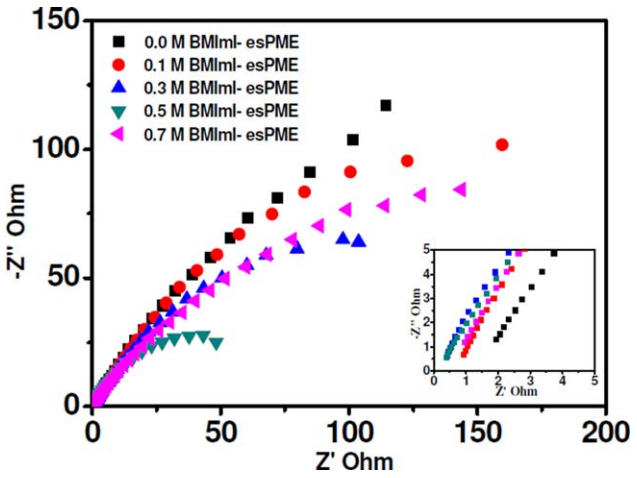

Figure 3. Nyquist plots for various concentrations of BMImI embedded esPMEs. [Color figure can be viewed in the online issue, which is available at wileyonlinelibrary.com.]

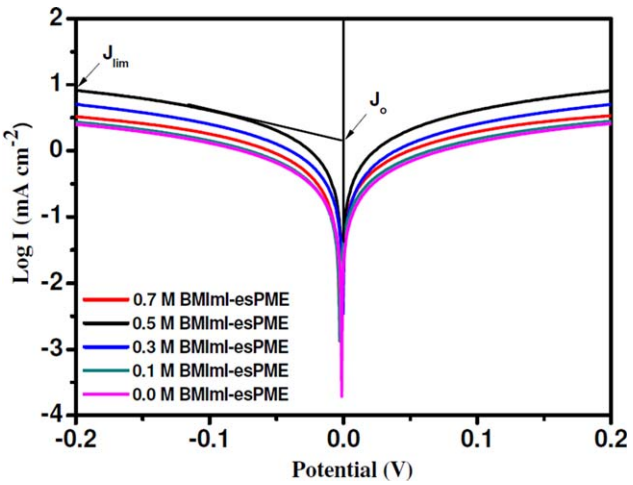

Figure 4. Tafel polarization curves for symmetrical cells fabricated with various concentrations of BMImI embedded esPMEs. [Color figure can be viewed in the online issue, which is available at wileyonlinelibrary.com.]

various concentrations (0, 0.1, 0.3, 0.5, and 0.7*M*) of BMImI (Figure 2). It was observed that the diffusion coefficient of triiodide increases as the concentration of BMImI increases up to a maximum of 0.5*M*. Beyond this concentration, the diffusion coefficient of I_3^-/I^- decreases (Table I). This is due to mass transfer limitations imposed by viscosity of ionic liquid. At 0.5*M* BMImI, the formation of I_3^- is favored which leads to higher cathodic limiting current than at other concentrations. Significantly, the cathodic limiting current for the redox couple increases linearly with respect to the concentration of BMImI, suggesting that physical diffusion may play major contributions in attaining high diffusion coefficient values. Increasing the concentration of BMImI beyond 0.5*M* decreases the diffusion coefficient of redox couple due to the higher viscosity of ionic liquid electrolyte which retards the ionic diffusion and also the formation of blocking layer at the TiO_2/electrolyte interface due to increased π-π stacking interactions.[31]

Ionic Conductivity Studies

The power conversion efficiency (PCE) of DSSCs depend on the ionic conductivity of the polymer matrix, which in turn depends on the charge carrier transfer and diffusion efficiency of the redox couple that are affected by the concentration of the ionic liquid, porosity of the esPM, electrolyte uptake, etc. In the case of imidazolium-based ionic liquids, as the length of the alkyl group increases, the ionic conductivity decreases[32] and the charge transport properties of imidazolium cation with a short alkyl chain of $<C_4$ should facilitate the diffusion of I_3^- in the electrolyte.[33] Indeed, BMImI has high short circuit current (J_{sc}) and increasing the chain length from C4 to C8 drastically decreases efficiency by decreasing the fill factor and short circuit photocurrent.[34] Nyquist plots of various concentrations of pure and BMImI-containing esPMEs are shown in Figure 3. The ionic conductivity of pure esPME is 1.103 × 10^{-3} S cm^{-1}. With the addition of BMImI in the esPME the ionic conductivity linearly increases to 5.830 × 10^{-3} S cm^{-1} for the system containing 0.5*M* BMImI (Figure 3 and Table II) and then decreases to 2.27 × 10^{-3} S cm^{-1} at 0.7*M* BMImI. The obtained ionic conductivity value for 0.5*M* BMImI containing esPME is higher than the values reported for other ionic liquid-containing esPMEs.[15–17] The incorporation of BMImI reduces the crystallinity of the esPME which increase the ionic conductivity up to 0.5*M* BMImI containing esPME. Beyond this concentration (>0.5*M* BMImI) the ionic conductivity decreases for

Table II. Influence of the Various Concentrations of BMImI in the Electrospun PVdF-HFP Membrane Electrolyte on Ionic Conductivity?

Electrolyte	Ionic conductivity (×10^{-3} S cm^{-1})
esPME	1.103
0.1*M* BMIml-esPME	2.249
0.3*M* BMIml-esPME	5.180
0.5*M* BMIml-esPME	5.830
0.7*M* BMIml-esPME	2.270

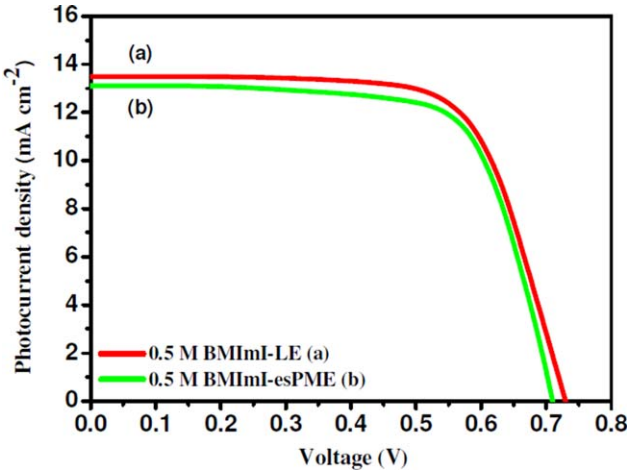

Figure 5. Photocurrent density–voltage (*J*–*V*) curves for the DSSC containing a) 0.5*M* BMImI-LE, b) 0.5*M* BMImI-esPME. [Color figure can be viewed in the online issue, which is available at wileyonlinelibrary.com.]

Table III. Photovoltaic Performance of the DSSCs Based on 0.5*M* BMImI-LE and 0.5*M* BMImI-esPME

Electrolyte	J_{sc} (mA cm^{-2})	V_{oc} (V)	FF	Cell efficiency (%)
0.5*M* BMImI-LE	13.49	0.73	71	6.99
0.5*M* BMImI-esPME	13.10	0.71	69	6.42

0.7*M* BMImI-esPME. This is due to the accumulation of more cations that results in increasing the crystallinity and an increase in viscosity that retards the ionic diffusion.[35] The porous structure of the esPMEs appears to improve ionic conductivity partly due to improved contact properties between the electrodes.[36–38]

Tafel Polarization Studies

Tafel-polarization curves were used to determine the electrocatalytic activity of the various concentrations of BMImI-esPMEs using dummy cells composed of FTO/Pt/BMImI-esPME/Pt/FTO (Figure 4). From the Tafel and the diffusion zones information was obtained on the exchange current density (J_o) and limiting diffusion current density (J_{lim}), which are closer to the catalytic activity of the electrode and electrolyte interface. The values of J_o can be obtained from the intersection of linear cathodic and anodic region and the values of J_{lim} can be obtained from the intersection of log I axis. A larger slope in the anodic and cathodic curves indicates a higher exchange current density (J_o) and better electrocatalytic activity towards the redox couple in the polymer membrane electrolyte. The enhancement in the J_o value for the 0.5*M* BMImI-containing esPME is in good agreement with the ionic conductivity values (Table II). The higher J_o and J_{lim} of the 0.5*M* BMImI-esPME is due to a larger diffusion coefficient value which offers faster reduction of I_3^- on the surface of catalyst expediting the diffusion of I_3^- ions. This consequently increased the Jsc value and the cell performance.

Photovoltaic Performance Studies

DSSCs were assembled using the 0.5*M* BMImI-esPME and the 0.5*M* BMImI-LE as a control to establish the role of the polymer electrolyte with respect to photovoltaic performance. Photocurrent density–voltage (J–V) curves obtained at a light intensity of 100 mW cm^{-2} under standard global AM 1.5 irradiation are shown in Figure 5 and in Table III. The DSSC fabricated using BMImI containing esPME shows the higher PCE than the other reported ionic liquids such as DMPImI and PMImI embedded esPMEs (Table IV). This can be explained by considering the charge transport and charge recombination effects of DSSC. On increasing the alkyl chain length from C4 to C8 of imidazolium cation decreases the PCE is due to the less diffusion coefficient of I_3^- resulting from its high viscosity. On the other hand, decreasing the alkyl chain length below C4 of imidazolium cation, increases the diffusion coefficient of I_3^- but decreases the electron recombination time which decreases J_{sc} and V_{oc} values. Hence, the chosen ionic liquid, BMImI fulfilling the requirements of high diffusion coefficient and increased electron recombination time to show higher PCE of the DSSC. Furthermore, both J_{sc} and FF were influenced by the ionic conductivity of the BMImI-containing esPME with the higher conductivity resulting an increase in charge transport and a decrease in charge transfer resistance.[33,34] The DSSC assembled with the 0.5*M* BMImI-esPME provides an energy conversion efficiency of 6.42%, which is close in value to that of the DSSC with the 0.5*M* BMImI-LE (6.99%). The relatively higher PCE for 0.5*M* BMImI-esPME is due to its high diffusion co-efficient of I_3^-/I^- and also high ionic conductivity of BMImI containing esPME.

Stability Studies

The J–V curves of the DSSCs employing the 0.5*M* BMImI-esPME and the 0.5 BMImI-LE were recorded over a period of 30 days. The variations in light to electricity conversion efficiency for the two DSSCs are shown in Figure 6. The cell efficiency was measured every 48 h after storage in the dark at 30°C. The normalized efficiency of the DSSC containing the 0.5*M* BMImI-LE decreased gradually and retained ~95% of its initial value after 30 days, whereas the DSSC based on the 0.5*M* BMImI-esPME retains ~99% of its initial value. It is interesting to note that no decay was observed in the overall power conversion efficiency of DSSC with the 0.5*M* BMImI-esPME even after 30 days. The esCPME offers the advantages of cohesive properties of the gel polymer electrolyte along with the diffusive nature of the liquid electrolyte due to its interconnected pores that can easily entrap a large quantity of liquid electrolyte which improves an excellent contacting and filling properties between the dye-adsorbed TiO_2 electrode and Pt counter electrode. This interconnected pore structure ensures the retention of the electrolyte and also prevent the leakage/evaporation of the electrolyte in esPME. Thus, the durability of the DSSC is increased tremendously than other conventional membrane electrolytes.[39] However, the BMImI-LE failed this because of its less retain capacity or gradual leakage/evaporation.

Table IV. Comparison Between Different Ionic Liquids Containing esPMEs on Ionic Conductivity and Photovoltaic Performance

Electrolyte	Ionic conductivity (S cm^{-1})	J_{sc} (mA cm^{-1})	Cell efficiency (%)	Reference
DMPImI—esPVdF-HFP	0.0013×10^{-3}	6.028	3.13	15
PMImI—esPVdF-HFP	4.53×10^{-3}	12.30	5.21	16
PMImI—esPVdF-HFP/PS	1.89×10^{-3}	11.60	5.75	17
0.5*M* BMImI-esPME	5.83×10^{-3}	13.10	6.42	Present study
0.5*M* BMImI-LE	7.69×10^{-3}	13.49	6.99	Present study

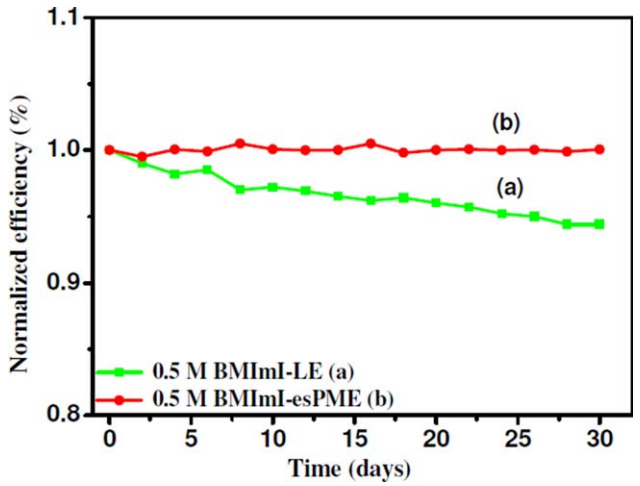

Figure 6. Normalized light-to electricity conversion efficiency of the DSSC containing a) 0.5*M* BMImI-LE, b) 0.5*M* BMImI-esPME. [Color figure can be viewed in the online issue, which is available at wileyonlinelibrary.com.]

CONCLUSIONS

An esPM incorporated with 0.5*M* BMImI containing liquid electrolyte was prepared and found to have a maximum diffusion co-efficient of 9.05 × 10^{-4} cm^2 S^{-1}. The 0.5*M* BMImI-esPME was used in the assemble of a DSSC giving an energy conversion efficiency of 6.42%, which is nearly the same as a DSSC assembled with a 0.5*M* BMImI-LE (6.99%) at an illumination intensity of 100 mW cm^{-2}. The stability of the DSSC assembled with the BMImI-esPME was considerably superior to that assembled with the 0.5*M* BMImI-LE.

ACKNOWLEDGMENTS

The authors gratefully acknowledge the CSIR (Ref. No.01/2359/10/EMR-II), New Delhi, for their financial support.

REFERENCES

1. Wang, P.; Zakeeruddin, S. M.; Moser, J.-E.; Grätzel, M. *J. Phys. Chem. B* **2003**, *107*, 13280.
2. Ganapatibhotla, L. V. N. R.; Zheng, J.; Roy, D.; Krishnan, S. *Chem. Mater.* **2010**, *22*, 6347.
3. Fei, Z.; Dyson, P. J. *Chem. Commun. (Camb).* **2013**, *49*, 2594.
4. Park, S. J.; Yoo, K.; Kim, J.-Y.; Kim, J. Y.; Lee, D.-K.; Kim, B.; Kim, H.; Kim, J. H.; Cho, J.; Ko, M. J. *ACS Nano* **2013**, *7*, 4050.
5. Freitas, F. S.; de Freitas, J. N.; Ito, B. I.; De Paoli, M. -A.; Nogueira, A. F. *ACS Appl. Mater. Interfaces* **2009**, *1*, 2870.
6. Wu, C.; Jia, L.; Guo, S.; Han, S.; Chi, B.; Pu, J.; Jian, L. *ACS Appl. Mater. Interfaces* **2013**, *5*, 7886.
7. Jeon, S.-H.; Priya, A. R. S.; Kang, E.-J.; Kim, K.-J. *Electrochim. Acta* **2010**, *55*, 5652.
8. Vijayakumar, G.; Lee, M. J.; Song, M.; Jin, S.-H.; Lee, J. W.; Lee, C. W.; Gal, Y.-S.; Shim, H. J.; Kang, Y.; Lee, G.-W.; Kim, K.; Park, N.-G.; Kim, S. *Macromol. Res.* **2009**, *17*, 963.
9. Zhang, R.; Ma, P. X. *J. Biomed. Mater. Res.* **1999**, *44*, 446.
10. Yang, C.-C.; Lin, C.-T.; Chiu, S.-J. *Desalination* **2008**, *233*, 137.
11. Martin, C. R. *Chem. Mater.* **1996**, *8*, 1739.
12. Ondarçuhu, T.; Joachim, C. *Europhys. Lett.* **1998**, *42*, 215.
13. Priya, A. R. S.; Subramania, A.; Jung, Y.-S.; Kim, K.-J. *Langmuir* **2008**, *24*, 9816.
14. Feng, L.; Li, S.; Li, H.; Zhai, J.; Song, Y.; Jiang, L.; Zhu, D. *Angew. Chem. Int. Ed. Engl.* **2002**, *41*, 1221.
15. Park, J.-Y.; Lee, J.-W.; Park, K. H.; Kim, T.-Y.; Yim, S.-H.; Zhao, X. G.; Gu, H.-B.; Jin, E. M. *Polym. Bull.* **2013**, *70*, 507.
16. Kim, J.-U.; Park, S.-H.; Choi, H.-J.; Lee, W.-K.; Lee, J.-K.; Kim, M.-R. *Sol. Energy Mater. Sol. Cells* **2009**, *93*, 803.
17. Park, S.-H.; Won, D.-H.; Choi, H.-J.; Hwang, W.-P.; Jang, S.; Kim, J.-H.; Jeong, S.-H.; Kim, J.-U.; Lee, J.-K.; Kim, M.-R. *Sol. Energy Mater. Sol. Cells* **2011**, *95*, 296.
18. Dao, V.-D.; Hoa, N. T. Q.; Larina, L. L.; Lee, J.-K.; Choi, H.-S. *Nanoscale* **2013**, *5*, 12237.
19. Ding, J.; Li, Y.; Hu, H.; Bai, L.; Zhang, S.; Yuan, N. *Nanoscale Res. Lett.* **2013**, *8*, 9.
20. Veerappan, G.; Kwon, W.; Rhee, S.-W. *J. Power Sources* **2011**, *196*, 10798.
21. Park, J. H.; Jun, Y.; Yun, H.-G.; Lee, S.-Y.; Kang, M. G. *J. Electrochem. Soc.* **2008**, *155*, F145.
22. Lee, K. S.; Jun, Y.; Park, J. H. *Nano Lett.* **2012**, *12*, 2233.
23. Huddleston, J. G.; Visser, A. E.; Reichert, W. M.; Willauer, H. D.; Broker, G. A.; Rogers, R. D. *Green Chem.* **2001**, *3*, 156.
24. Subramania, A.; Sundaram, N. T. K.; Sathiya Priya, A. R.; Kumar, G. V. *J. Membr. Sci.* **2007**, *294*, 8.
25. Arora, P.; Zhang, Z. J. *Chem. Rev.* **2004**, *104*, 4419.
26. Angulakshmi, N.; Stephan, A. M. *Electrochim. Acta* **2014**, *127*, 167.
27. Cui, Y.; Zhang, X.; Feng, J.; Zhang, J.; Zhu, Y. *Electrochim. Acta* **2013**, *108*, 757.
28. Suryanarayanan, V.; Lee, K.-M.; Chen, J.-G.; Ho, K.-C. *J. Electroanal. Chem.* **2009**, *633*, 146.
29. Salam, Z.; Vijayakumar, E.; Subramania, A. *RSC Adv.* **2014**, *4*, 52871.
30. Subramania, A.; Vijayakumar, E.; Sivasankar, N.; Sathiya Priya, A. R.; Kim, K.-J. *Ionics* **2013**, *19*, 1649.
31. Kubo, W.; Kitamura, T.; Hanabusa, K.; Wada, Y.; Yanagida, S. *Chem. Commun.* **2002**, 374.
32. Suryanarayanan, V.; Lee, K.-M.; Ho, W.-H.; Chen, H.-C.; Ho, K.-C. *Sol. Energy Mater. Sol. Cells* **2007**, *91*, 1467.
33. Kubo, W.; Kambe, S.; Nakade, S.; Kitamura, T.; Hanabusa, K.; Wada, Y.; Yanagida, S. *J. Phys. Chem. B* **2003**, *107*, 4374.

34. Zafer, C.; Ocakoglu, K.; Ozsoy, C.; Icli, S. *Electrochim. Acta* **2009**, *54*, 5709.

35. Kim, J. R.; Choi, S. W.; Jo, S. M.; Lee, W. S.; Kim, B. C. *Electrochim. Acta* **2004**, *50*, 69.

36. Wang, Y. *Sol. Energy Mater. Sol. Cells* **2009**, *93*, 1167.

37. Jeong, S.-K.; Jo, Y.-K.; Jo, N.-J. *Electrochim. Acta* **2006**, *52*, 1549.

38. Yang, R.; Zhang, S.; Zhang, L.; Liu, W. *Int. J. Electrochem. Sci.* **2013**, *8*, 10163.

39. Singh, P. K.; Bhattacharya, B.; Mehra, R. M.; Rhee, H.-W. *Curr. Appl. Phys.* **2011**, *11*, 616.